J Mater Sci: Mater Electron (2013) 24:4958–4963
DOI 10.1007/s10854-013-1507-5

Growth of CZTS thin films by sulfurization of sputtered single-layered Cu–Zn–Sn metallic precursors from an alloy target

Shanshan Zhou · Ruiqin Tan · Xin Jiang · Xiang Shen · Wei Xu · Weijie Song

Received: 19 July 2013 / Accepted: 25 September 2013 / Published online: 13 October 2013

Abstract Cu_2ZnSnS_4 (CZTS) thin films were prepared by sulfurizing single-layered metallic Cu–Zn–Sn precursors which were deposited by DC magnetron sputtering using a Cu–Zn–Sn ternary alloy target. The composition, microstructure and properties of the CZTS thin films prepared under different sputtering pressure and DC power were investigated. The results showed that the sputtering rate of Cu atom increases as the sputtering pressure and DC power increased. The microstructure of CZTS thin films can be optimized by sputtering pressure and DC power. The CZTS thin film prepared under 1 Pa and 30 W showed a pure Kesterite phase and a dense micro-structure. The direct optical band gap of this CZTS thin film was calculated as 1.49 eV with a high optical absorption coefficient over 10^4 cm^{-1}. The Hall measurement showed the film is a p-type semiconductor with a resistivity of 1.06 Ω cm, a carrier concentration of 7.904×10^{17} cm^{-3} and a mobility of 7.47 cm^2 Vs^{-1}.

1 Introduction

The compound semiconductor Cu_2ZnSnS_4 (CZTS) thin film has attracted much attention recently due to its potential use in cost effective thin film solar cells. CZTS has a high absorption coefficient above 10^4 cm^{-1} and a direct band gap of 1.40–1.50 eV [1, 2]. Its crystalline structure is commonly referred to as the Kesterite type. This structure is strongly related to the Chalcopyrite structure of well known photovoltaic absorber material $Cu(In,Ga)Se_2$ with the record efficiency of 20.3 % [3]. Furthermore, all the constituents in CZTS are abundant in the crust of the earth and are nontoxic. The excellent properties make them to be promising candidates for photovoltaic materials.

At present, 8.4 ± 0.2 % conversion efficiency from a CZTS-based solar cell has been reported [4]. In the case of CZTS solar cells incorporation selenium, a conversion efficiency of 11.1 ± 0.3 % has been obtained [5], which is well below its theoretical conversion efficiency of 32.2 % [6]. A pure CZTS absorption layer with a dense microstructure is the key factor to prepare high efficiency solar cells. CZTS thin films have been prepared by several methods, such as sulfurization of sputtered [7–12] or evaporated [13] precursor films, spray method [14, 15], sol–gel method [16], solvothermal approach [17], hydrazine deposition [5], electrode deposition [18] and co-evaporation [19]. Among these methods, wet chemical ways are highly dependent on the reaction environment and material proportion, for example solvothermal approach, sol–gel method and so on. Even worse, some methods need to use toxic chemicals, for example hydrazine deposition. Magnetron sputtering is an environment-friendly method to prepare high quality and large-area thin films with good controllability and repeatability compared with these wet chemical ways. There have been some reports about $Cu(In,Ga)Se_2$ films prepared by sputtering of quaternary $Cu(In,Ga)Se_2$ alloy target [20, 21]. The use of the alloy target to produce metallic precursors offers some advantages, such as uniform large scale

S. Zhou · R. Tan (✉) · X. Shen
College of Information Science and Engineering, Ningbo University, Ningbo 315211, People's Republic of China
e-mail: tanruiqin@nbu.edu.cn

X. Jiang
Lanzhou Institute of Chemical Physics, Chinese Academy of Sciences, Lanzhou 730000, People's Republic of China

W. Xu · W. Song
Ningbo Institute of Material Technology and Engineering, Chinese Academy of Sciences, Ningbo 315201, People's Republic of China

fabrication, easily adjustable compositions, and process simplification compared to the fabrication using multiple targets or multilayer precursors.

In this study, we demonstrate the growth of CZTS films using a simple approach based on DC magnetron sputtering with a Cu–Zn–Sn alloy ternary target to deposit single-layered metallic precursors following a sulfurization process. The effects of the sputtering pressure and DC power on the composition, crystallographic phase, microstructures, morphology of Cu–Zn–Sn precursors and CZTS films were investigated. Furthermore, the optical and electrical properties of the obtained films in relation to their potential for photovoltaic applications were discussed.

2 Experimental details

CZTS thin films were prepared by a two-stage method. At the first stage, Cu–Zn–Sn metallic precursors were deposited onto Mo-coated soda lime glass (SLG; 2 cm × 2 cm × 3 mm) by DC magnetron sputtering system using a Cu–Zn–Sn ternary alloy target (5 × 5 cm^2) with an atomic ratio 5:3:2. The purities of Cu, Zn, Sn were 99.99 %. The thickness of Mo layer is 1 μm. The base vacuum of the sputter chamber was evacuated below 3 × 10^{-4} Pa. The substrates were rinsed in acetone, methanol and deionized water ultrasonically, then dried with nitrogen gas. The sputtering pressure and power were selected as Table 1. An approximately 600–900 nm-thick Cu–Zn–Sn metallic precursor was obtained by sputtering 50 min.

At the second stage, the metallic precursors were sulfurized in a GSL1600X-II type dual-zone tube furnace enclosed with elemental sulfur powder (5 N). Before starting the heating power, the tube was applied 15 min Ar after evacuation. The flux of Ar was fixed at 50 sccm controlled by a mass flow controller. The sulfur powder zone was heated to 200 °C and maintained. For the Cu–Zn–Sn precursor zone, the temperature of the substrate was first maintained at 200 °C for 10 min to homogenize the precursors. Then, the precursors were sulfurized at 550 °C for 30 min in the flux of S_2(gas) + Ar, followed by natural cooling after the reaction period.

The structural property of the samples was examined using X-ray diffraction (XRD, Bruker AXSD8 Advance), using a CuK_α radiation source ($\lambda = 1.5406$ Å). Raman scattering measurements was performed with a confocal Raman spectrometer (Raman, Renishaw inVia micro-Raman system) excited by Ar^+ laser with wavelength of 488 nm. The film composition and morphology were determined by energy dispersive spectroscopy (EDS, Hitachi S4800) and scanning electron microscope (SEM, Hitachi S4800).The surface roughness was investigated by Scanning Probe Microscopy (AFM, CSPM 5500). The optical and electrical properties were analyzed by UV–VIS spectrophotometer (PerkinElmer Lambda 950) and Hall measurements (UK Accent HL5500 PC), respectively.

3 Results and discussion

3.1 Compositional and structural properties

Table 1 shows the composition ratio of each element in metallic precursors and CZTS thin films, determined by EDS. Compared the composition ratio of Cu in metallic precursors A–E, it is clear that the sputtering rate of Cu increases as the sputtering pressure and DC power increases. For the obtained CZTS films sulfurized at 550 °C for 30 min, the composition ratio of sulfur reaches about 50 % showing the achievement of the sufficient sulfurization. As the previous report [22], the sulfurization process performed under vacuum conditions causes losses of Zn in the elemental form and Sn in the sulfide compound form. For our work, the ratios of Cu/(Zn + Sn) in sulfurized films were increased compared with that in their precursors. In contrast, the ratio of Zn/Sn was decreased. From this behavior, we consider that at higher temperatures the re-evaporation of zinc and tin compounds may be happened. In comparison, the changing rate of zinc was obvious than the others.

The crystallinity quality and grain orientation of the thin films were investigated by XRD, shown in Fig. 1. For all the sulfurized thin films, the peaks of 2θ = 28.53°, 32.99°, 47.33°, 56.17°, 76.44° can be attributed to the diffraction of

Table 1 The chemical compositions of various precursors and CZTS thin films

Sample name	DC power (W)	Sputtering pressure (Pa)	CZT precursors			CZTS thin film		
			Cu	Cu/(Zn + Sn)	Zn/Sn	S/(Cu + Zn + Sn)	Cu/(Zn + Sn)	Zn/Sn
A	30	0.3	44.1	0.79	1.53	1.11	0.84	0.99
B	30	0.7	45.9	0.85	1.49	1.20	0.91	1.12
C	30	1.0	47.4	0.9	1.27	1.05	1.01	0.98
D	20	1.0	44.8	0.81	1.87	0.98	1.09	1.31
E	40	1.0	48.2	0.93	1.24	1.05	1.21	0.90

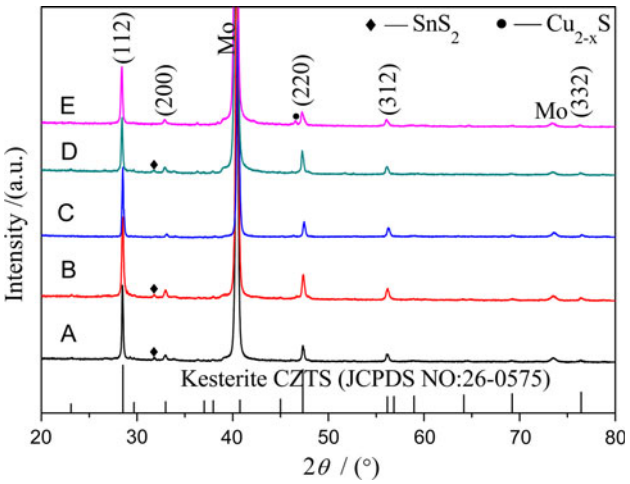

Fig. 1 XRD patterns of CZTS thin films on Mo-coated SLG substrate

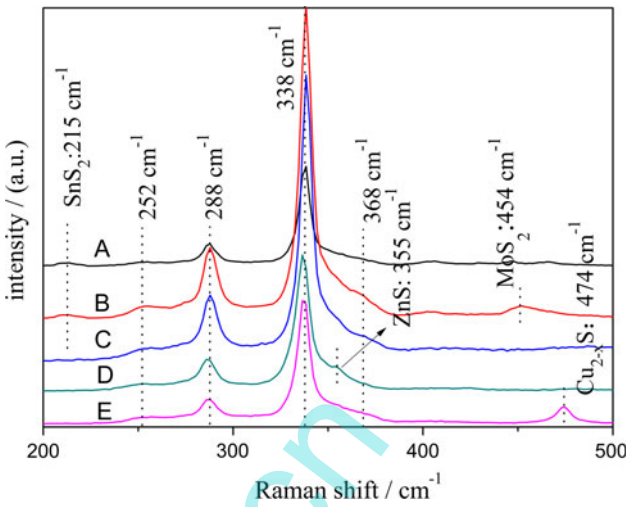

Fig. 2 Raman scattering spectra of CZTS thin films on Mo-coated SLG substrate

(112), (200), (220), (312) and (332) planes of Kesterite structure CZTS (JCPDS NO: 26-0575). The weak peak at $2\theta = 31.73°$ in sample A, B and D was the main peaks of SnS_2 (JCPDS NO: 40-1467). According to the EDS there is no excess of Sn atoms in the metallic precursors. We consider that the SnS_2 may be caused by the Sn atoms local enrichment in the metallic precursors of sample A, B and D. Meanwhile, there is a obvious peak of $Cu_{2-x}S$ (JCPDS NO: 23-0958) at $2\theta = 46.45°$ in sample E. It is attributed to excess of Cu atoms shown in Table 1. However, no peaks relat-ed to SnS_2 and $Cu_{2-x}S$ compounds shows in the diffraction patterns of the CZTS sample C (1.0 Pa, 30 W). In addition, XRD measurements showed that all CZTS films were grown well with (112)—oriented crystalline texture. Because the unit cell parameters of cubic-ZnS, tetragonal-Cu_2SnS_3, cubic-Cu_2SnS_3 are quite similar to that of CZTS (a: 5.435 Å, c: 10.843 Å), their spectra are very similar for visible peaks and their angle differences are within the instrument accuracy. Raman scattering measurements were carried out to confirm these XRD results.

The result of Raman scattering analysis is presented in Fig. 2. It's clear to see that all the samples have four main peaks of CZTS at 252, 288, 338, and 368 cm^{-1}, which are in agreement with previous reports [23]. In addition, fingerprints of SnS_2 were observed by the presence of a minor peak at 215 cm^{-1} [12] for sample A, B and the $Cu_{2-x}S$ peak at 474 cm^{-1} [23] for sample E, respectively. All of these are in accordance with XRD patterns except for sample D. The fingerprints of ZnS were observed by the presence of minor peak at 355 cm^{-1} [24, 25] in Raman spectra of sample D. This can be explained by the significant excess of Zn atoms both in the metallic precursor and the sulfurized film, shown in Table 1. The Raman spectra of sample C shows the evidence of the formation of CZTS single phase without any cubic-ZnS, tetragonal-Cu_2SnS_3, cubic-Cu_2SnS_3 characteristic modes.

3.2 Morphological and micro-structure properties

From Fig. 3 we can remark that the root-mean-square average (RMS) roughness value of CZT precursor films decreases as sputtering pressure increase from 0.3 to 1.0 Pa or as DC powers increase from 20 to 40 W. The former is attributed to the probability of collisions between work gas and sputtered particles increases as the sputtering pressure increases. The sputtered particles have enough energy to diffuse which results in the formation of more compact films. The latter may be related to two factors. Firstly, the power density of the target is enhanced as well as the kinetic energy and the migration ability of the sputtered particles (Cu, Zn, Sn) as the DC power increasing, which results in the increase of diffusion distance of the particles as they reach the substrates. Secondly, the calorific value of the target improves and the actual irradiation to the substrates enhances as the power density of the target increasing, which improve the migration capabilities of the atoms in the film.

Figure 4A1–E1 shows the SEM surface photographs of the CZTS sample A–E, respectively. The corresponding AFM images of each sample are shown in the right-hand images (Fig. 4A2–E2). The RMS roughness of the sulfurized CZTS thin films ranging from 30 to 66 nm are larger than that of CZT precursor films ranging from 4.4 to 12.3 nm, which shows the evidence of the grain sizes of the films increased after sulfurization. From the SEM results, we can see some voids distributed in the surface of sample A, B and D, which is agreement with the previous reports [10]. The formation of voids could be due to the

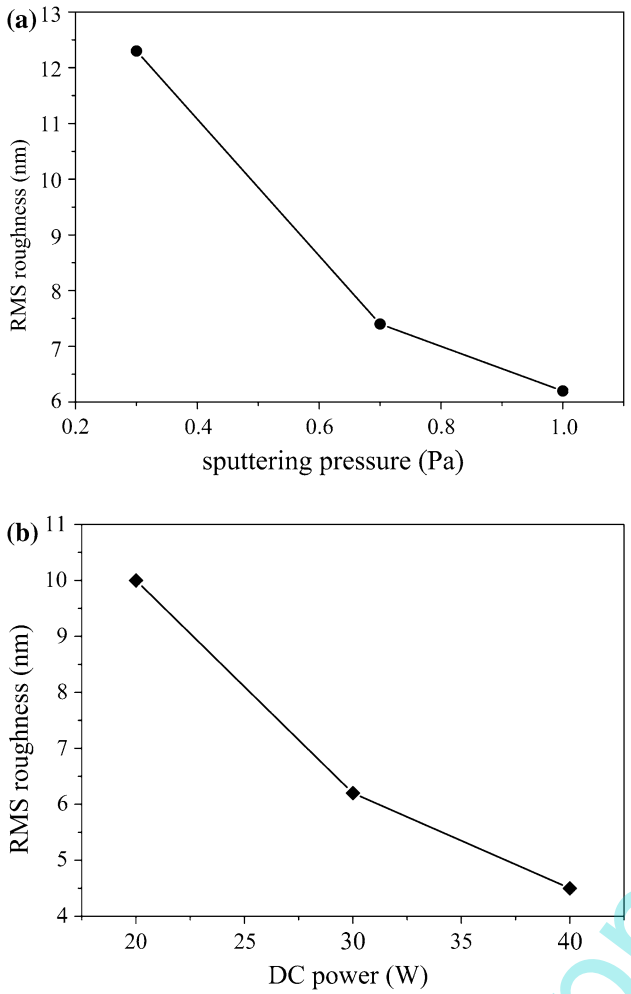

Fig. 3 RMS roughness of CZT precursor films prepared by different sputtering pressures (**a**) and DC powers (**b**)

sublimation of elemental or binary compounds at a lower evaporation temperature such as Zn and SnS_x during annealing. The presence of voids may cause a path for leakage current, which tend to degrade the absorber layer quality. Sample C and E have compact surfaces without any holes but the RMS roughness of them are larger than other samples'. We consider that the re-evaporation of tin and zinc from the film surface was greatly restrained as the sample sulfurized from a dense and smooth precursor film. In the sulfurization process, the compact structure of sample C and E promoted the formation of much bigger grains (Fig. 4C1, E1) which led to their larger RMS roughness values (Fig. 4C2, E2). The big grains in sample E were $Cu_{2-x}S$ determined by EDS, which was attributed to the excess of Cu atoms in the precursor. From the above results, it is concluded that the microstructures of CZTS thin films can be determined by the RMS roughness and chemical compositions of the precursor films, which can be optimized by sputtering pressure and DC power.

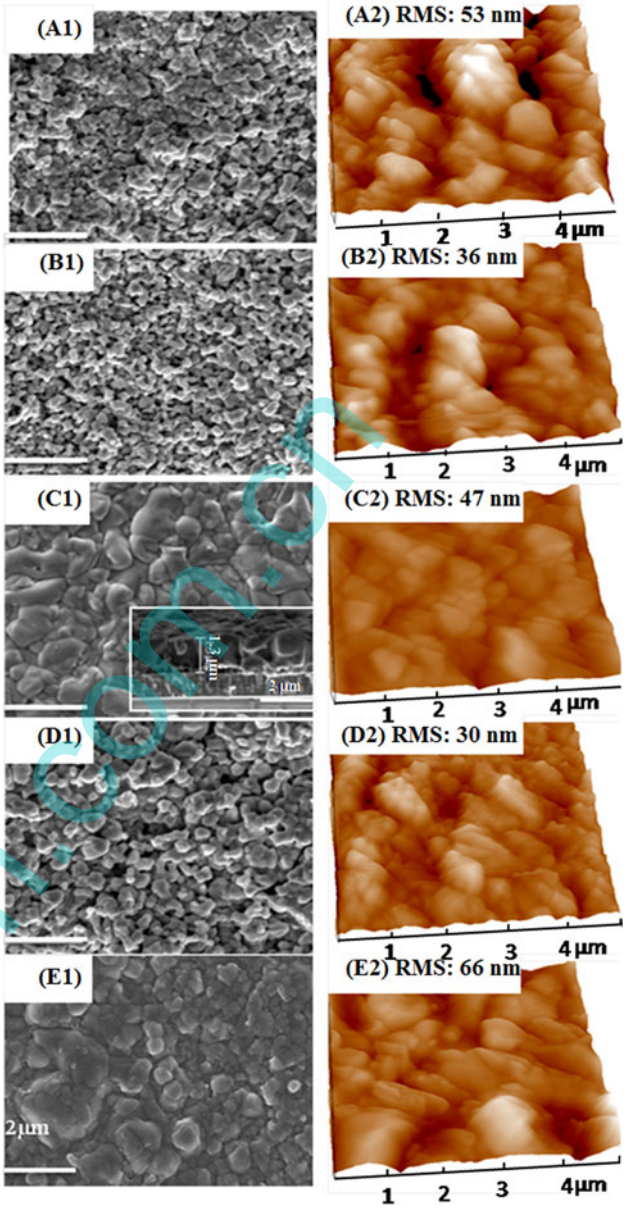

Fig. 4 Surface morphology images and 3D-AFM images of CZTS thin films

From the cross-section of the film as shown in Fig. 4C1 inset picture, it can be seen that the film obtained with 30 W and 1.0 Pa consists of closely packed columnar grains which are approximately 1 μm wide. It should be remarked that columnar grains extending from the bottom to the top of the CZTS layer. The grains have sizes similar to the film thickness (1.3 μm). This feature is similar to that of CZTS films prepared by thermal evaporation in a vacuum system leading to the highest conversion efficiency of 8.4 % [4], and beneficial to decreasing the minority carrier recombination during transport process when applied to solar cell.

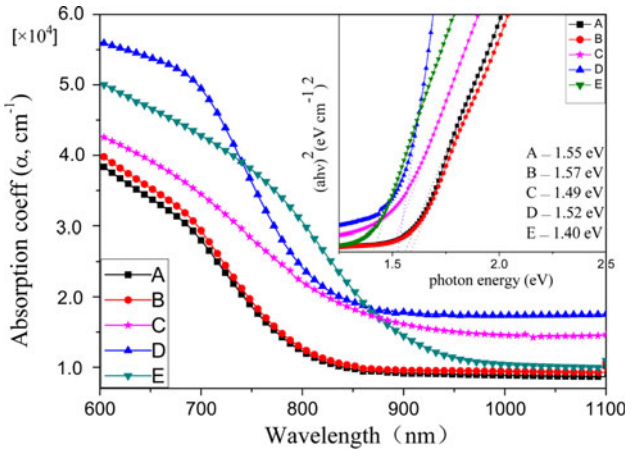

Fig. 5 Absorption coefficient spectra of CZTS samples *A–E*. (The *inset* shows the energy band gap of CZTS thin films)

3.3 Optical and electrical properties

Figure 5 shows the absorption coefficient versus wavelength for the fabricated CZTS thin films, which were evaluated by measuring the transmittance spectra in the wavelength range of 600–1,100 nm using the UV–VIS spectrophotometer. All CZTS thin films show a high optical absorption coefficient larger than 10^4 cm^{-1}. The band gap values were estimated from the $(ah\nu)^2$ versus $(h\nu)$ plots by extrapolating the linear part of the function as shown in inset of Fig. 5. The obtained band gaps range from 1.40 to 1.57 eV for CZTS sample A–E, which is consistent with the result of the previous reports [11, 26]. It was known that the band gap energy of ZnS, SnS_2 and $Cu_{2-x}S$ was about 3.65, 2.6 and 1.21 eV, respectively. These secondary phases in the CZTS samples resulted in the narrow or wide optical band gap energy as compared to ideal value [27, 28]. The obtained CZTS thin films can absorb the photon energy consisting of the visible and infrared rays, which is well matched to the solar spectrum. The band gap value of sample C (1.49 eV) is quite close to the theoretical optimal value for a single-junction solar cell [29].

The electrical properties of CZTS thin films determined by Hall measurements. The theory of Hall measurements base on Hall effect. The Hall voltage of CZTS thin films were calculated using the equation of:

$$U_H = R_H \frac{I_S B}{d} = \frac{1}{ne} \frac{I_S B}{d} \quad (1)$$

therefore carrier concentration can be calculated by:

$$n = \frac{I_S B}{U_H e d} \quad (2)$$

where $R_H = \frac{1}{ne}$is the Hall coefficient, B is the applied magnetic field (0.53 T), I_S is the electric current, d is the thickness of the CZTS film, n is the carrier concentration, e is the elementary charge.

Table 2 Results of the Hall effect measurements of the CZTS thin films

Sample name	Resistivity (Ω cm)	Carrier concentration (cm^{-3})	Mobility (cm^2 Vs^{-1})	Hall voltage (V)
A	0.8418	6.030×10^{18}	1.23	6.86×10^{-6}
B	0.6209	2.556×10^{18}	3.93	9.19×10^{-6}
C	1.057	7.904×10^{17}	7.47	4.88×10^{-5}
D	0.5976	2.754×10^{19}	0.379	1.77×10^{-6}
E	0.4307	1.246×10^{19}	1.16	1.70×10^{-5}

The relationship of the resistivity (ρ), the carrier concentration (n), and Hall mobility (μ), is given by the following equation:

$$\rho = \frac{1}{ne\mu} \quad (3)$$

Table 2 shows the electrical properties of CZTS thin films. The result showed that all the samples with $U_H > 0$, exhibited p-type semiconductor material characteristics. The resistivity, carrier concentration and Hall mobility are between the ranges of 0.43–1.06 Ω cm, 7.904×10^{17}–2.754×10^{19} cm^{-3}, and 0.379–7.47 cm^2 Vs^{-1}, respectively. This was similar to the result of Ref. [29]. Sample D and E has the lower resistivity and the highest carrier concentration. This result was caused by the presence of ZnS and $Cu_{2-x}S$, which are high conductivity materials [11, 30]. The mobility of CZTS thin films was dependant on the microstructure and impurity of thin film. For sample D, small grains caused by excess of Zn and the voids in the films are the reason of low electrical mobility. In addition, the sample C with the single phase of CZTS and dense microstructure exhibited higher electrical mobility, which can meet the requirements for the applications in thin film solar cells.

4 Conclusions

In this study, a facile preparation method of the CZTS thin films was provided by sulfurization of single-layered metallic precursors sputtered using single Cu–Zn–Sn ternary alloy target. The sputtering rate of Cu atom increases as the sputtering pressure and DC power increase. A pure CZTS thin film with a compact and good crystalline microstructure obtained by the sputtering pressure at 1.0 Pa and DC power at 30 W. The direct optical band gap of this CZTS thin film was calculated as 1.49 eV with a high optical absorption coefficient over 10^4 cm^{-1}. The Hall measurement showed this *p*-type semiconductor thin film with a resistivity of 1.06 Ω cm, a carrier concentration of 7.904×10^{17} cm^{-3} and a mobility of 7.47 cm^2 Vs^{-1}. All

the optical and electrical properties indicate that the CZTS film prepared by DC magnetron sputtering deposition using a Cu–Zn–Sn ternary alloy target is very promising material as absorber layer of thin film solar cells.

Acknowledgments This work is supported by the National Science Foundation of China (No. 21377063), the Ningbo Natural Science Foundation (No. 2012A610120), K.C. Wong Magna Fund in Ningbo University and "Information and Communication Engineering" Priority Discipline Open Fund of Zhejiang Province.

References

1. J.M. Raulot, C. Domain, J.F. Guillemoles, J. Phys. Chem. Solids **66**, 2019 (2005)
2. H. Katagiri, K. Jimbo, W.S. Maw, K. Oishi, M. Yamazaki, H. Araki, A. Takeuchi, Thin Solid Films **517**, 2455 (2009)
3. P. Jackson, D. Hariskos, E. Lotter, S. Paetel, R. Wuerz, R. Menner, W. Wischmann, M. Powalla, Prog. Photovolt. Res. Appl. **19**(7), 894 (2011)
4. B. Shin, O. Gunawan, Y. Zhu, N.A. Bojarczuk, S.J. Chey, S. Guha, Prog. Photovolt. Res. Appl. **1**, 72 (2013)
5. T.K. Todorov, J. Tang, S. Bag, O. Gunawan, T. Gokmen, Y. Zhu, D.B. Mitzi, Adv. Energy. Mater. **3**, 34 (2013)
6. W. Shockley, H.J. Queisser, J. Appl. Phys. **32**, 510 (1961)
7. F.Y. Liu, Y. Li, K. Zhang, C. Yan, Y.Q. Lai, Z. Zhang, J. Li, Y.X. Liu, Sol. Ener. Mat. Sol. C. **94**(12), 2431 (2010)
8. J.S. Seol, S.Y. Lee, J.C. Lee, H.D. Nam, K.H. Kim, Sol. Ener. Mat. Sol. C. **75**, 155 (2003)
9. T. Tanaka, T. Nagatomo, D. Kawasaki, M. Nishio, Q.X. Guo, A. Wakahara, A. Yoshida, H. Ogawa, J. Phys. Chem. Solids **66**(11), 1978 (2005)
10. N. Momose, M.T. Htay, T. Yudasaka, S. Lgarashi, T. Seki, S. Lwano, Y. Hashimoto, K. Ito, Jpn. J. Appl. Phys. **50**, 1 (2011)
11. M. Ikhlasul Amal, K.H. Kim, J. Mater. Sci. Mater. Electron **24**, 559 (2013)
12. P. Fernandes, P. Salomé, A. Da Cunha, J. Alloy. Compd. **509**(28), 7600 (2011)
13. A. Weber, H. Krauth, S. Perlt, B. Schubert, I. Kötschau, S. Schorr, H.W. Schock, Thin Solid Films **517**, 2524 (2009)
14. N. Nakayama, K. Ito, Appl. Surf. Sci. **92**, 171 (1996)
15. Y.B. Kishore Kumar, P. Uday Bhaskar, G. Suresh Babu, V. Sundara Raja, Phys. Status Solidi. (a) **207**, 149 (2010)
16. K. Tanaka, M. Oonuki, N. Moritake, H. Uchiki, Sol. Ener. Mat. Sol. C. **93**, 583 (2009)
17. Q.W. Tian, X.F. Xu, L.B. Han, M.H. Tang, R.J. Zou, Z.G. Chen, M.H. Yu, J.M. Yang, J.Q. Hu, CrystEngComm **14**, 3847 (2012)
18. A. Ennaoui, M. Lux-Steiner, A. Weber, D. Abou-Ras, I. Kötschau, H.-W. Schock, R. Schurr, A. Hölzing, S. Jost, R. Hock, T. Voβ, J. Schulze, A. Kirbs, Thin Solid Films **517**, 2511 (2009)
19. K. Oishi, G. Saito, K. Ebina, M. Nagahashi, K. Jimbo, W.S. Maw, H. Katagiri, M. Yamazaki, H. Araki, A. Takeuchi, Thin Solid Films **517**, 1449 (2008)
20. Y.C. Lin, Z.Q. Lin, C.H. Shen, L.Q. Wang, C.T. Ha, C. Peng, J. Mater. Sci. Mater. Electron **23**, 493 (2012)
21. P. Fan, J. Chi, G. Liang, X. Cai, D. Zang, Z. Zheng, P. Cao, T. Chen, J. Mater. Sci. Mater. Electron **23**, 1957 (2012)
22. P.A. Fernandes, P.M.P. Salome, A.F. da Cunha, Thin Solid Films **517**, 2519 (2009)
23. H. Yoo, J.H. Kim, Thin Solid Films **518**, 6567 (2010)
24. M. Grossberg, J. Raudoja, K. Timmo, M. Altosaar, T. Raadik, Thin Solid Films **519**, 7403 (2011)
25. Y.M. Yu, M.H. Hyun, S. Nam, D. Lee, O. Byungsung, K.S. Lee, P.Y. Yu, Y.D. Choi, J. Appl. Phys. **91**, 9429 (2002)
26. S.W. Shin, J.H. Han, C.Y. Park, S.R. Kim, Y.C. Park, G.L. Agawane, A.V. Moholkar, J.H. Yun, C.H. Jeong, J.Y. Lee, J.H. Kim, J. Alloys. Compd. **541**, 192 (2012)
27. C. Khélia, K. Boubaker, T. Ben Nasrallah, M. Amlouk, S. Belgacem, J. Alloy. Compd. **477**, 461 (2009)
28. S.W. Shin, S.M. Pawar, C.Y. Park, J.H. Yun, J.H. Moon, J.H. Kim, J.Y. Lee, Sol. Ener. Mater. Sol. Cells **95**, 3202 (2011)
29. J. Zhang, Y.J. Fu, D. Shao, L. Shao, Acta Sci. Natur. Univ. Sunyatseni, **46**(z1), 32 (2007)
30. H. Katagiri, N. Ishigaki, T. Ishida, Jpn. J. Appl. Phys. **40**, 500 (2001)